AD-A097 600 NATIONAL AERONAUTICS AND SPACE ADMINISTRATION CLEVEL--ETC F/G 11/6
EFFECTS OF GEOMETRIC VARIABLES ON RUB CHARACTERISTICS OF TI-6AL--ETC(U)
APR 81 R C BILL, J WOLAK, D W WISANDER
UNCLASSIFIED NASA-E-449 NASA-TP-1835 NL

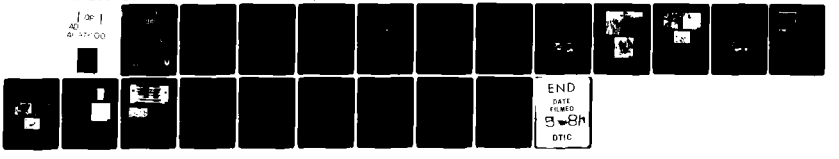

NASA
Technical Paper 1835

AVRADCOM
Technical Report 80-C-19

LEVEL II

Effects of Geometric Variables on Rub Characteristics of Ti-6Al-4V

Robert C. Bill, Jan Wolak,
and Donald W. Wisander

APRIL 1981

NASA

NASA
Technical Paper 1835

AVRADCOM
Technical Report 80-C-19

Effects of Geometric Variables on Rub Characteristics of Ti-6Al-4V

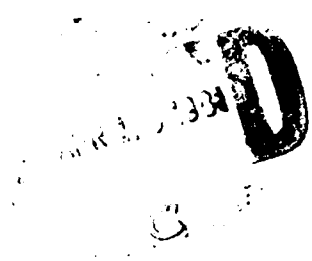

Robert C. Bill
Propulsion Laboratory
AVRADCOM Research and Technology Laboratories
Lewis Research Center
Cleveland, Ohio

Jan Wolak
University of Washington
Seattle, Washington

Donald W. Wisander
Lewis Research Center
Cleveland, Ohio

National Aeronautics
and Space Administration

**Scientific and Technical
Information Branch**

1981

Summary

Experiments simulating rub interactions between Ti-6Al-4V blade tips and various seal materials were conducted. Rub conditions investigated included single- and 10-blade-tip interactions, reduced-thickness blade tips, and deliberately rounded blade tips. The blade tips were rotated at 114 m/sec, and the seal material was driven into the rotating blade tips at 25.4×10^{-6} m/sec. Experiments were conducted in air at room temperature. Seal materials included porous, sintered metals and plasma-sprayed, metal-based materials. Contact was found to be quite unsteady for all combinations except those incorporating deliberately rounded blade tips. The unsteady contact was characterized by long periods of rubbing contact and increasing blade tip load that terminated in sudden rapid metal removal, sometimes accompanied by tearing and disruption of porous seal material under the rub surface. A model describing the blade tip loading is proposed and is based on the propagation of an elastic stress wave through the seal material as the seal material is dynamically compressed by the blade tip leading edge. The model incorporates blade tip leading-edge geometric features, experimental conditions of rub speed and incursion rate, and seal material properties.

Symbols

a	velocity of sound in seal material, m/sec
D	depth of incursion per blade pass, m
E	modulus of elasticity of seal material, MN/m^2
F_r	total radial load on blade tip, N
$f(\xi)$	impulse function, N
$g(t)$	unit impulse function, $sec^{1/2}/m$
K	stiffness of load cell cantilever, N/m
L	measured radial load, N
l	blade tip thickness, m
m	effective mass of load cell cantilever, kg
N	number of blade tips
r	radius of curvature of blade tip leading edge, m
t	time, sec
Δt	impulse time, sec
V	blade tip velocity, m/sec
W	blade tip width, m
x	distance in sliding direction from leading edge to any point on blade tip, m
$y(t)$	displacement of load cell cantilever, m
$\dot{\Delta}$	incursion rate, m/sec
ρ	blade tip leading-edge radius of curvature (sharpness), m
σ	radial stress acting on blade tip, N/m^2
σ_1	stress acting on leading edge of blade tip, N/m^2
τ	period of impulse, or blade tip contact interval (fig. 15)
τ_f	friction torque, N-m
ω	rotational speed of blade tip rotor, rad/sec
ω_n	natural frequency of load cell cantilever, rad/sec

Introduction

The efficiency of gas turbine engines is strongly dependent on clearances between stationary gas-path seal components and rotating blade tips or labyrinth seal knife edges. Very significant reductions in thrust specific fuel consumption are realizable if minimum gas-path seal clearances are maintained throughout the engine (refs. 1 and 2). Operating with minimal clearances inevitably results in rubs between the rotating and stationary components due to thermal response effects, dynamic loading, and engine flexibility. Such rubs, occurring as they do at extremely high speeds (typically 300 to 400 m/sec), can result in destructively high temperatures, wear to the rotating components, and unpredictable behavior of the gas-path seal material comprising the static component.

To maintain engine efficiency and structural integrity, wear should occur to the static component (gas-path seal material) rather than to the rotating component. Gas-path seal materials are designed and structured so as to preferentially undergo wear and thus minimize wear to the rotating component in the event of a rub interaction.

Previous rub interaction studies have been conducted on a variety of gas-path seal materials, but the rotating materials and configurations have not been systematically varied. In references 3 and 4 the

effects of controlled variations in the composition and microstructure of low-density, sintered gas-path seal materials were studied, and phenomenological rub behavior models were proposed. Various plasma-sprayed materials with and without deliberately introduced porosity were evaluated in reference 5, and a promising new compressor seal system based on porous, plasma-sprayed aluminum bronze was identified. Experimental studies of the rub characteristics of open-face honeycomb materials were reported in reference 6. In the studies occurrence of thermoelastic instabilities was observed on the rotor, and abrasive rotor wear attributable to braze-rich areas was noted.

In the present study experimental variations in the configuration of the simulated rotating blade tip system are evaluated. In particular, the number of blade tips, the blade tip dimensions, and the leading-edge sharpness were varied. Other experimental parameters including rub speed, incursion rate, and incursion depth were held constant. One of the objectives was to identify the influence of blade tip configurations on the mechanisms of blade tip-seal material interactions. Further development of a blade tip load analytical model was also an objective, with the role of blade tip geometry and seal material properties being a primary consideration in the model.

Experiments were conducted in air at room temperature with Ti-6Al-4V as the blade tip material and with 21-percent-dense, sintered Hastelloy-X fibermetal as the seal material in most cases. Experiments were also conducted with sintered, 40-percent-dense Nichrome and plasma-sprayed nickel-graphite, aluminum-graphite, and aluminum-polyester coatings. Blade tip velocity was 114 m/sec, the incursion rate was 25.4×10^{-6}, and the standard incursion depth was nominally 630 micrometers. For the plasma-sprayed coatings the incursion depth was 500 micrometers.

Apparatus

Rub evaluations were conducted on the apparatus shown in figure 1. A complement of either one or 10 simulated blade tips was rotated at velocities to 114 m/sec. Drive power was provided by a 2.24-kilowatt induction motor coupled to a continuous-speed variator that permitted control of the rub speed.

Simulated blade tip specimens were 12.7 millimeters wide, and two blade tip thicknesses were evaluated: a standard thickness of 3.2 millimeters, and a reduced thickness of 0.8 millimeter. Also, some standard-thickness blade tips were provided with a rounded tip of about 6 millimeters radius of curvature, the axis of curvature of the rounded trip being perpendicular to the sliding direction. Otherwise all blade tips were evaluated in an as-ground condition, for which the leading-edge sharpness was about 5 micrometers (radius of curvature). The grinding direction was perpendicular to the sliding direction.

The gas-path seal material sample was mounted on a slideway feed mechanism so that it could be driven radially into the rotor. A radial incursion rate of 25.4×10^{-6} m/sec was employed.

During a rub interaction test radial loads and frictional torque were continuously recorded, and an infrared pyrometer was used to monitor and record individual blade tip temperatures. Radial loads were sensed by means of strain gages applied to the gas-path seal material sample support. A torque transducer in the shaft system, located between the speed variator and the bearing spindle directly behind the disk, provided frictional torque data. The infrared pyrometer, located 90° past the rub contact as shown in figure 1, indicated the number of blade tips participating in the rub interaction per revolution as well as the temperature.

Wear debris generated during the rub interaction was collected on the fixture shown in figure 1. Debris particles impinged on a strip of sticky tape and thus were captured for subsequent examination and evaluation. Optical microscopy, scanning electron microscopy (SEM), and energy dispersive X-ray analysis (EDAX) were used to study the rub debris.

A dial gage indicator showed the relative radial motion of the feed slideway carriage with respect to the rotating disk. Incursion depths could be controlled to within 25 micrometers of the desired depth. Usually a 630-micrometer incursion depth was employed.

Procedure

Before testing, the blade tips were ground to a 0.5-micrometer finish (except for the specially rounded tips) so that the tip surface was as nearly parallel as possible to the supporting root. The tips were then cleaned with ethanol, and the height of each simulating blade tip was measured. Height variations were maintained to within 4 micrometers. The specially rounded tips were prepared by a hand-finishing process employing 400-grit paper backed up by a segment of 12.7-millimeter-inside-diameter tubing.

Blade tips were assembled onto the wheel in complements of either 10 active blade tips or one active blade tip. The 10-tip complement was achieved by leaving two blade tip positions on the wheel (out of the 12 positions) vacant, one of the two left vacant having been improperly broached. The single-active-

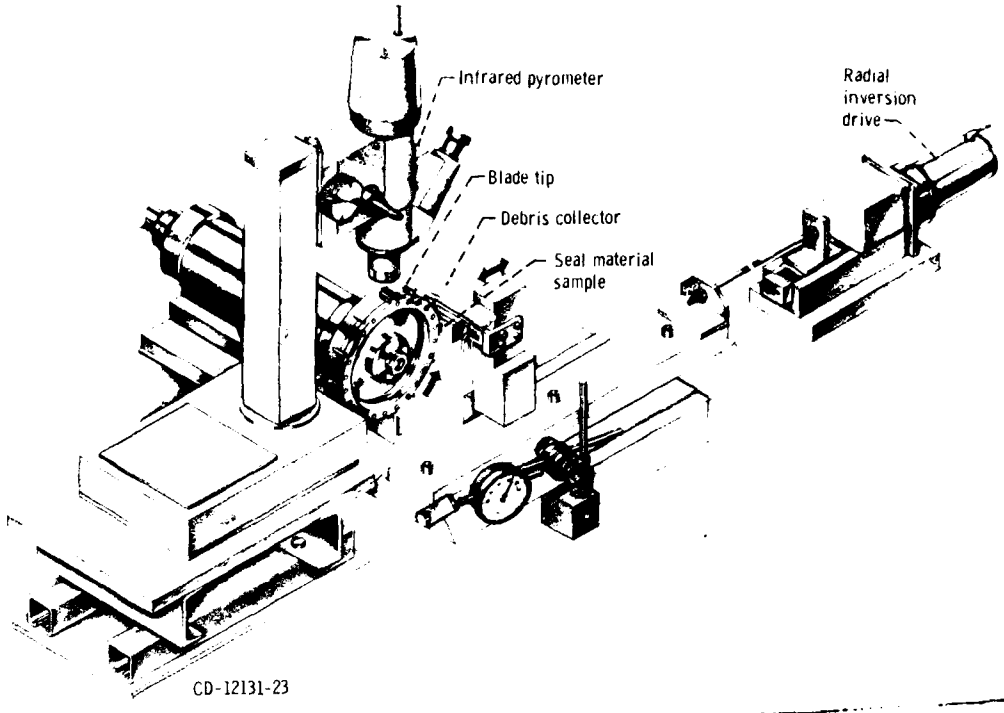

(a) Test apparatus.

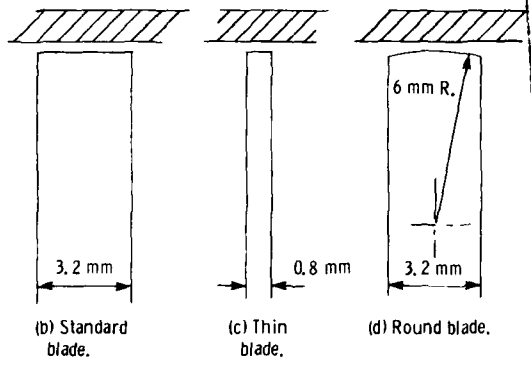

(b) Standard blade. (c) Thin blade. (d) Round blade.

Figure 1. - Test apparatus and sections through blade tips.

blade-tip complement employed a short "dummy" blade tip diametrically opposite the active tip for dynamic balance purposes. In all cases the rounded blade tips were assembled in the single-active-tip configuration.

Selected gas-path seal material samples were epoxy bonded to a mild-steel backing that was fastened to a combination specimen support and cantilever load cell. The rotor was brought to the desired rotating speed, the selected incursion rate was set, and the rub interaction was begun. In these tests the interaction was continued to a 630-micrometer depth.

A blade tip velocity of 114 m/sec was selected for this study. The incursion rate employed was 25.4×10^{-6} m/sec.

Post-test evaluation included microscopic examination of blade tip and abradable material rub surfaces and examination of wear debris. A measure of the wear (or transfer) to the blade tip leading edges was obtained by observing specimen focal plane

height changes over the tip surface during microscopic examination.

Materials

Blade tips were fabricated from the titanium alloy Ti-6Al-4V (titanium-6 percent aluminum-4 percent vanadium) in the solution-treated, age-hardened condition (hardness of Rockwell C32). This particular alloy is representative of materials used for compressor blades and labyrinth seal components in current gas turbine engines.

Five gas-path seal materials representing the current state of the art were used in these experiments. The majority of the experiments were conducted on one of these materials, namely, 21-percent-dense, sintered Hastelloy-X fibermetal.

The 21-percent-dense (79 percent open porosity) Hastelloy-X fibermetal consisted of r. ·l fibers 100 to 150 micrometers in length and 10 micrometers in diameter sintered together in a loose, open structure. This material has a nominal tensile strength of 12 MPa. The hardness on the Rockwell 15Y (R_{15Y}) scale was below zero.

Another sintered material was also used in these experiments; it consisted of Nichrome (Ni-20Cr) particles 75 to 100 micrometers in diameter sintered to approximately 40 percent density. The tensile strength of this material was about 4 MPa. Again, the hardness was below zero on the R_{15Y} scale.

In addition to the sintered materials three plasma-sprayed, gas-path seal materials were subjected to rub experiments. The first of these was, by composition, nickel-25-volume-percent graphite. In the as-sprayed condition the hardness of this material was R_{15Y} 10.

A composite plasma-sprayed coating consisting of an aluminum-12-percent-silicon alloy with a 40-percent-by-volume addition of polyester was also employed in this study. This material was rubbed in the as-sprayed condition, for which its hardness was R_{15Y} 62.

Finally, experiments were conducted on a plasma-sprayed aluminum-graphite coating in the as-sprayed condition. The hardness of this coating was R_{15Y} 34.

Results

The results of the rub interaction experiments are summarized in tables I and II. For comparison the baseline configuration was taken to be the one incorporating 10 blade tips with a thickness of 3.2 millimeters and an initial leading-edge sharpness (radius of curvature) of about 5 micrometers. The baseline seal material is 21-percent-dense, sintered Hastelloy-X fibermetal. The effects of varying the number of blade tips, the blade tip thickness, the leading-edge sharpness, and the seal material are described separately.

Number of Blade Tips

As shown in table I reducing the number of 3.2-millimeter-thick blade tips from the baseline 10 to one had an effect on peak loads and torques. The unsteady nature of the radial load for single blade-tip

TABLE I. – Ti-6Al-4V BLADE TIPS AGAINST SINTERED HASTELLOY-X FIBERMETAL

Number of blade tips, N	Blade tip thickness, l, mm	Leading-edge sharpness, ρ, μm	Steady radial load, L, N	Steady frictional torque, τ_f, N-m	Peak radial load, L, N	Peak frictional torque, τ_f, N-m	Condition of rub surface	Blade tip wear[a]
10	3.2	5	2.5	0.07	17	0.27	Smeared with frictional tearing	H1; M6
10	↓	↓	1.5-2.5	.16	10	.5	Smeared with frictional tearing	VH1; H2; M4
10	↓	↓	3.5-4.0	.32	10	.5	Smeared	VH3; M1; L6
1	↓	↓	[b]3.5-4.0	.1	7.5	.15	Smeared with frictional tearing	VH1 with transfer
1	↓	↓	[b]2.5	.12	12.5	.2	Smeared	VH1 with transfer
1	↓	↓	[b]3.5	.16	12.5	----	Smeared	VH1 with transfer
10	.8	↓	5.0	.18	10	.27	Smeared	H5; L2
10	.8	↓	3.5	----	3.5	----	Smeared with burnout	H3; L3
10	.8	↓	3.5-4.0	.13	4.0	.13	Smeared with burnout	H2; M3; L2
1	3.2	6×10^3	3.5-4.0	.12	7.5	.2	Smeared with burnout	Heavy transfer
1	3.2	6×10^3	5.0	.2	5.0	.25	Smeared	Heavy transfer
1	3.2	6×10^3	4.0	.16	4.0	.2	Smeared with burnout	Heavy transfer

[a]H means heavy leading-edge wear, 40 to 60 μm as measured at leading edge; M means medium leading-edge wear, 10 to 20 μm as measured at leading edge; VH means very heavy wear, about 80 μm or more as measured at leading edge; L means light wear, < 10 μm as measured at leading edge.

[b]Unsteady load pattern; "steady" load difficult to define.

TABLE II. Ti-6Al-4V BLADE TIPS AGAINST VARIOUS SEAL MATERIALS

[Leading-edge sharpness, ρ, 5 μm.]

Seal material	Number of blade tips, N	Blade tip thickness, t, mm	Steady radial load, L_r, N	Steady frictional torque, τ_f, N-m	Peak radial load, L_r, N	Peak frictional torque, τ_f, N-m	Condition of rub surface	Blade tip wear
Sintered NiCr	10	3.2	0	0	2	0.05	Slight smearing (10 percent of surface)	M3, L6
Sintered NiCr	10	8	0.5-1	.03	2.5	.10	Smearing over about 20 percent of surface	M1 + transfer
Sintered NiCr	1	3.2	0	0	7.5	.07	No smearing	M1
Ni-25-percent graphite	10	3.2	0	0	5	.03	Smearing over about 10 percent of surface	M1, L6
Ni-25-percent graphite	10	8	2.5	.02	10	.07	No smearing	M3, L7
Ni-25-percent graphite	1	3.2	0	0	10	.03	No smearing	H1
Aluminum-silicon-polyester	10	3.2	0	0	15	.10	Smearing over entire surface	H10
Aluminum-silicon-polyester	10	8	1.5	.03	3.5	.07	↓	Heavy transfer
Aluminum-silicon-polyester	1	3.2	0	0	5	.03		Heavy transfer
Aluminum-graphite	10	3.2	0	0	20	.15		Ridulation
Aluminum-graphite	1	3.2	0	0	10	.08		H1 + transfer

[a]H means heavy leading-edge wear, 40 to 60 μm as measured at leading edge; M means medium leading-edge wear, 10 to 20 μm as measured at leading edge; L means light leading-edge wear, < 10 μm as measured at leading edge.

tests, noted in table I, is illustrated in figure 2(a). There were time intervals during which no contact was indicated, and periods during which load peaks of 0.1- to 0.2-second duration and 5- to 15-newton magnitude were superimposed on rough, slowly increasing or decreasing background loads. In comparison 10-blade-tip tests (fig. 2(b)) typically showed a steady load of 2 to 4 newtons throughout most of the rub interaction, with peak loads of 0.5- to 1.0-second duration and about 10-newton amplitude toward the end of the test. The effect that reducing the number of blade tips had on steady torque was minor, although the peak torques recorded seemed to be somewhat lower, as noted in table I.

The condition of the rub surface on a sintered fibermetal specimen after a rub interaction with one blade tip is shown in figure 3; the rub surface was generally similar to this after interaction with 10 blade tips. Deep cracks and fissures penetrating through the smeared rub surface well into the porous substrate are in evidence. These cracks sometimes led to disruption of the smeared layer on a macroscopic scale, with exposure of the torn, porous substrate, as denoted by "frictional tearing" in table I. The cracks were a direct result of frictional stresses since they were oriented normal to the sliding direction. Thermal-stress-induced cracks can be seen on a much finer scale and show no preferential orientation.

Blade tip wear and transfer of seal material to the blade tips were both more intense in tests involving one blade tip than with 10. Representative blade tip photomicrographs from single- and 10-blade-tip interactions are shown in figure 4. Especially noticeable are the comparatively heavy deposits of transferred seal material (about 2 μm thick away from the leading edge) resulting from the single-blade-tip rub interactions and the formation of a leading-edge prow. Multiple-blade-tip tests resulted in a thinner, more uniform transferred layer, with no evidence of prow formation. Although the presence of transferred material made wear measurements uncertain, it was estimated that the depth of blade tip removal near the leading edge was about 50 percent greater for single-blade-tip tests than for 10-blade-tip tests. Thus the wear volume of a single blade tip was about twice that of any individual tip from a multiple (10)-blade test.

The rub debris collected from a single-blade-tip test is shown in figure 5. In comparison with debris from 10-blade-tip tests, significantly more of the particles appear to have been torn from the porous seal material without having been extensively smeared. Energy dispersive X-ray analysis indicates the presence of titanium in the rub debris from both single- and 10-blade-tip tests, and this is consistent with observe blade tip wear. The particles containing titanium were very fine and approximately spherical in shape as can be seen in figure 5(b).

Blade Tip Thickness

The effects of reducing blade tip thickness from 3.2 millimeters to 0.8 millimeter are summarized in

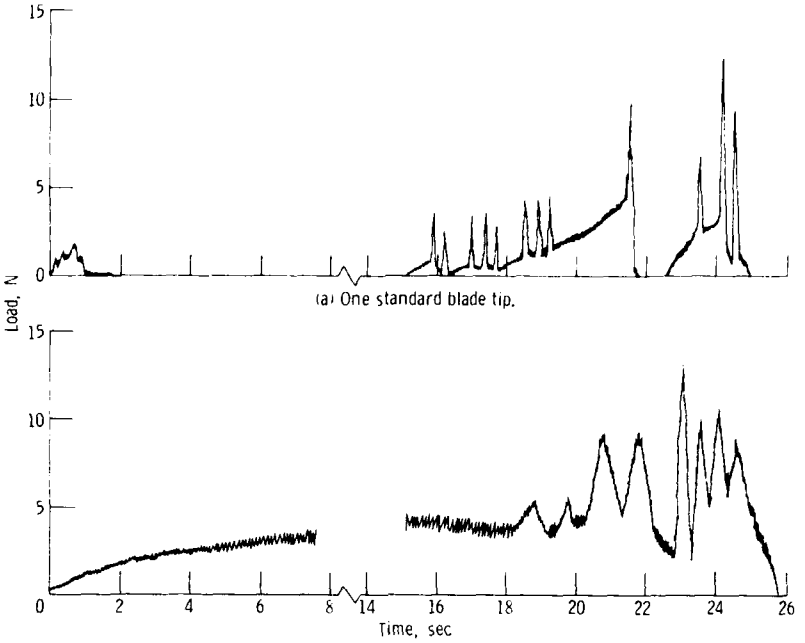

(b) Ten standard blade tips.

Figure 2. - Radial load as a function of time for rub interactions between one standard Ti-6Al-4V blade tip and sintered 21-percent-dense Hastelloy-X fibermetal, with 10-standard-blade-tip interaction shown for comparison.

Figure 3. - Sintered Hastelloy-X fibermetal seal surface after rub interaction with one Ti-6Al-4V blade tip. Blade tip velocity, 114 m/sec; incursion rate, $25 \cdot 10^{-6}$ m/sec.

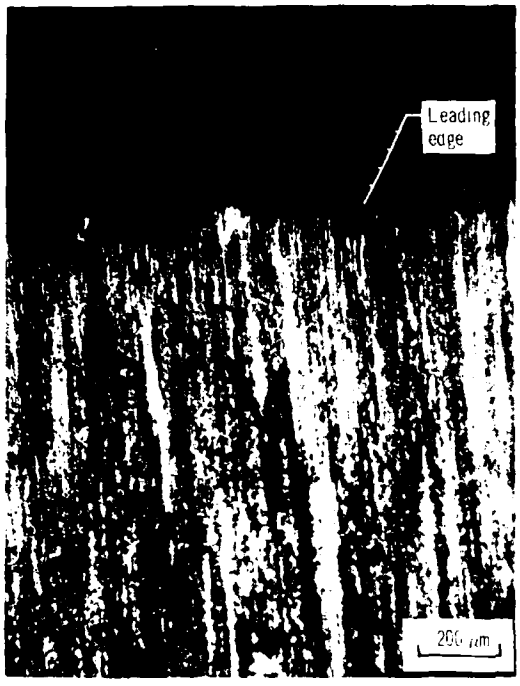

(a) Ten-blade-tip interaction.

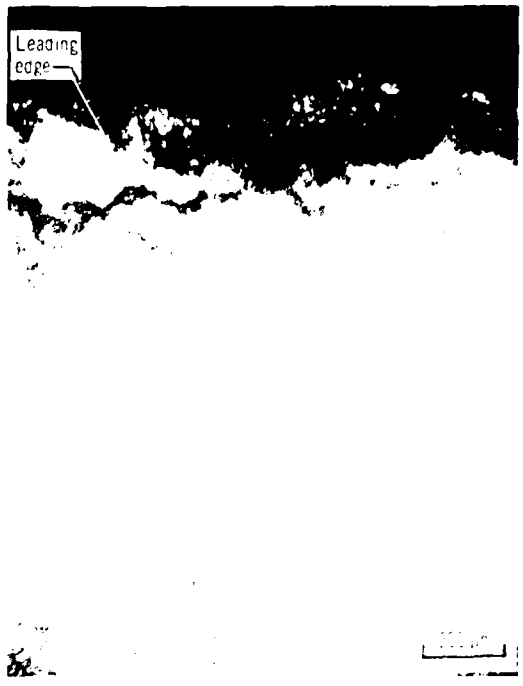

(b) One-blade-tip interaction.

(c) Scanning electron micrograph of transferred material near leading edge of single blade tip.

Figure 4. - Condition of blade tips after multiple (10) and single-blade-tip interactions.

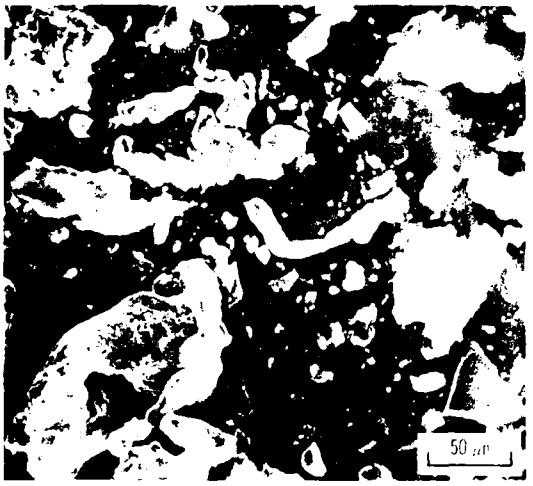

(a) Typical debris particles.

(b) Spherical debris particles.

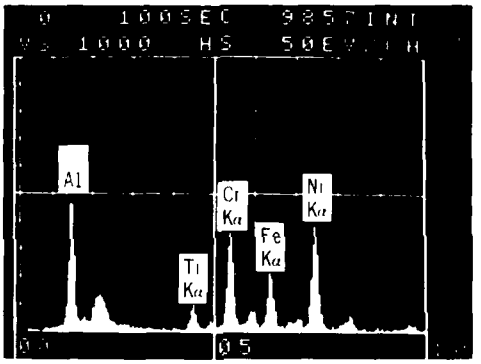

(c) Energy dispersive X-ray analysis of (b).

Figure 5. - Wear debris from rub interaction between a single Ti-6Al-4V blade tip and sintered, 21-percent-dense Hastelloy-X fibermetal. Blade tip velocity, 114 m/sec; incursion rate, 25.10-6 m/sec.

table I, and the effects on radial load are shown in figure 6. The radial load was more steady for the thin-blade-tip rub interactions, and the load peaks were either less severe or of longer duration. Steady torque was not affected by blade tip thickness, although peak torque amplitudes were reduced appreciably, as shown in table I.

The rub surface of a sintered Hastelloy-X fibermetal seal material specimen and a metallographic section through the rub groove after interaction with 10 thin blade tips are shown in figure 7. The rub surface was completely smeared, with cracks induced by friction, as was the case for the standard-thickness blade tip tests. The tendency for tearing of the smeared surface, however, was not as great for the thin-blade-tip tests. Sectioning the rub groove revealed the smeared "friction-affected layer," that layer adjacent to the rub surface showing obvious effects attributable to frictional heating (discoloration, fine cell structure), to be about 5 micrometers thick. There was another layer of densified fibermetal, about 30 micrometers thick, below the friction-affected layer. Hence densification of the fibermetal (which strain hardens) was nonuniform with depth and was constrained to a relatively shallow layer near the surface.

The condition of the thin blade tips after a rub interaction is represented by the photomicrograph in figure 8. Five to 10 micrometers of smeared, transferred seal material is present over nearly the entire blade tip. In addition to transfer, wear of the thin blade tip was in evidence. Blade tip wear was concentrated in scratches, about 10 to 20 micrometers deep, crossing the entire blade tip

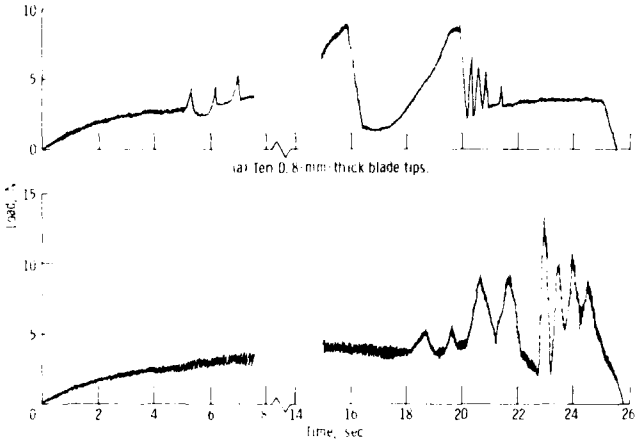

(a) Ten 0.8-mm-thick blade tips.

(b) Ten 3.2-mm-thick blade tips.

Figure 6. - Radial load as a function of time for rub interactions between 0.8-mm-thick Ti-6Al-4V blade tips and sintered, 21-percent-dense Hastelloy-X fibermetal, with standard-blade-tip interaction shown for comparison.

(a) Overview of smeared rub surface.

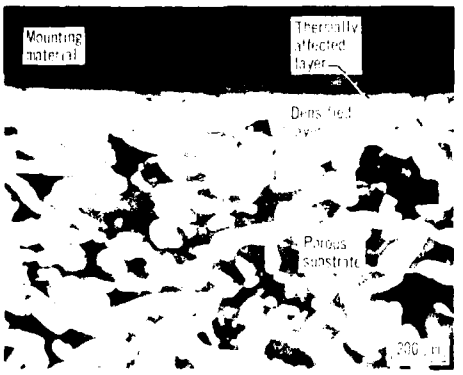

(b) Section through rub surface.

Figure 7. - Sintered, 21-percent-dense Hastelloy-X fibermetal after rub interaction against 10 thin Ti-6Al-4V blade tips. Blade tip velocity, 114 m/sec; incursion rate, 25×10^{-6} m/sec.

Figure 8. - Thin (0.8-mm thick) Ti-6Al-4V blade tip after rub interaction against 21-percent-dense Hastelloy-X fibermetal. Blade tip velocity, 114 m/sec; incursion rate, 25×10^{-6} m/sec; 10-blade interaction.

thickness over about 25 percent of the tip width. In addition, 30 to 40 micrometers of wear was evident at the blade tip leading edges. Altogether, the total volume of material removed from the thin blade tips was estimated to be 20 to 30 percent less than the volume of material removed from the 3.2-micrometer-thick blade tips.

Debris from rub tests between 10 thin T-6Al-4V blade tips and sintered Hastelloy-X fibermetal, shown in figure 9, was quite similar to that from rub tests with 10 standard-thickness blade tips (ref. 3). Flattened debris particles with a layered morphology are much in evidence and originate no doubt from the smeared rub surface invariably generated on the seal material. An important difference between the rub tests with the thin blade tips and those with the standard-thickness tips was the greater concentration of fine, spherical debris particles in the thin-blade-tip tests. Energy dispersive X-ray analyses again revealed that the fine particles contained titanium, an indication that they were from the blade tips.

Rounded Blade Tips

Rub interactions employing single blade tips with a 6-millimeter leading-edge sharpness (rounded tips) resulted in a load pattern that was qualitatively very different from that obtained when 5-micrometer leading-edge sharpness (standard tips) was employed. As shown in figure 10 the radial load was very smooth and uniform and gradually rose to a steady value of 5 newtons. The minor fluctuations shown are about 0.5-newton in amplitude, and the period of these fluctuations is about 60 milliseconds, corresponding to three or four rotations of the disk. In contrast, tests on a blade tip with 5-micrometer leading-edge sharpness show very erratic radial load patterns (fig. 10(b)).

The friction torque recorded for the rounded-blade-tip tests was also very smooth and continuous. Torque levels were slightly higher than those recorded for tests with two standard-sharpness blade tips but lower than the values recorded for the 10-blade-tip baseline tests.

The condition of the rub surface on the seal material specimen is shown in figure 11. Considerable heat discoloration is evident on the smeared portion of the rub groove, and the central part of the groove has been heavily oxidized (fig. 11(a)). The exposed fibermetal substrate in the central area displayed a brown discoloration caused by oxidation. On the smeared portion of the rub surface (fig. 11(b)) a thermocrack network is very much in evidence.

The rub debris was similar to that collected from tests on the baseline (10 blade tips) configuration. Most of the particles showed evidence of having originated from the smeared rub surface; other (fine) particles were found to be high in titanium content and to have come from the blade tips.

Seal material transferred to the rounded blade tips in the manner shown in figure 12. Titanium alloy was exposed at the crown of the blade tip, where tip wear was concentrated. A prow of seal material built up toward the leading edge, and a trailing swarf formed toward the trailing edge.

Rub Behavior Against Various Seal Materials

The number of blade tips and the blade tip thickness were varied in rub experiments against four seal materials in addition to Hastelloy-X fibermetal. The results of these experiments are summarized in table II. The thin-blade-tip configuration was the only configuration to give measurable steady loads and torques in these experiments. Peak loads were generally comparable in magnitude to those for Hastelloy-X fibermetal, with the lowest peak load observed for the sintered nickel-chromium material.

Those materials that did not smear appreciably (sintered nickel-chromium and plasma-sprayed nickel-graphite) showed a maximum peak load under single-blade-tip test conditions in the 3.2-millimeter-

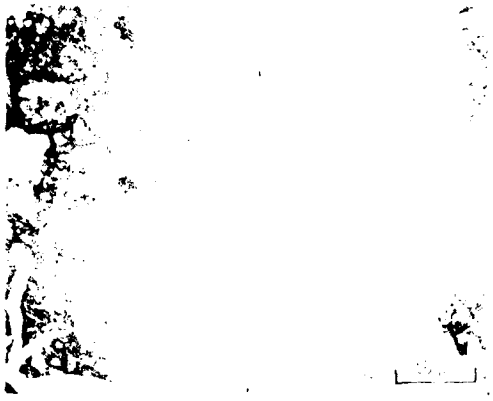

(a) Typical debris particles.

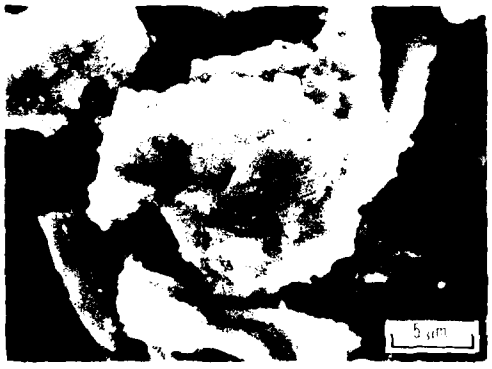

(b) Layered debris.

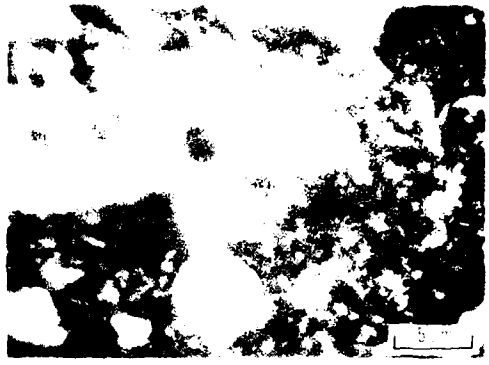

(c) Spherical debris.

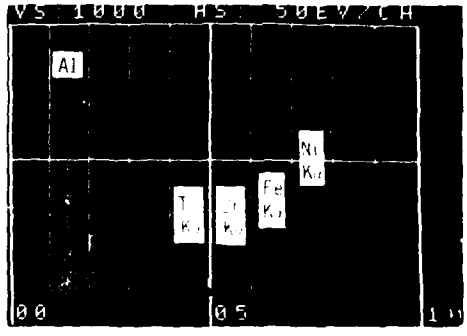

(d) Energy dispersive X-ray analysis of (c).

Figure 9. - Wear debris from rub interaction between thin (0.8-mm-thick) Ti-6Al-4V blade tips and 21-percent-dense Hastelloy-X fiber metal. Blade tip velocity, 114 m/sec; incursion rate, 25 $\cdot$ 10^{-6} m/sec; 10-blade interaction.

thick-blade-tip tests. A metallographic section through the nickel-graphite rub surface, shown in figure 13, indicates a cleanly abraded rub surface. In contrast, the highest peak load occurred in tests with 10 blade tips for those materials that showed significant smearing (the aluminum-based materials). Also, heavy transfer of seal material to the blade tips was observed after single-blade-tip experiments with the aluminum-based materials, the transfer being concentrated near the leading edge.

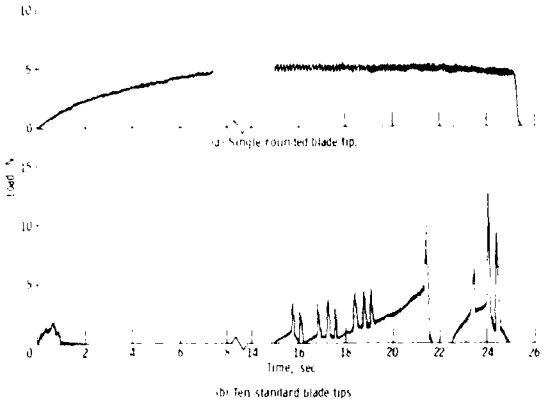

(a) Single rounded blade tip.

(b) Ten standard blade tips.

Figure 10. - Radial load as a function of time for rub interactions between rounded blade tip and 21-percent-dense Hastelloy-X fibermetal, with standard blade-tip interaction shown for comparison.

Discussion

By far the easiest and least expensive techniques of in-service seal shaping would be to permit sharp leading edges of the blade tips to cut the seal material. For this approach to be successful it is necessary that the blade material be harder than the seal material, at the temperature at which the cut is to be made, by at least 20 percent (ref. 7, p. 347). Should this condition be violated, the cutting edge would loose its sharpness soon after it came in contact with the work piece; and rubbing, instead of cutting, would take place with resultant high interface temperatures and loss of control of groove generation.

Besides the requirement that the blade tip retain a hardness at least 20 percent higher than that of the seal material, the radius of curvature (sharpness) of the tip leading edge must be small as compared with the depth of cut per blade pass (ref. 8). Expressed quantitatively, for the blade tips to function as efficient cutting tools

$$\rho < \frac{2\pi\dot{\Delta}}{\omega N} \tag{1}$$

where ρ is the radius of curvature of the leading edge, $\dot{\Delta}$ is the incursion rate, ω is the rotational speed, and N is the number of blade tips on the disk. For a disk as used in these experiments, equipped with 10 blade tips and rotating at 10 000 rpm, the radius of curvature should be less than 0.025 micrometer. In fact, the tip leading-edge sharpness after grinding is about 5 micrometers. Hence under most circumstances the character of blade tip interaction with the seal material would be expected to be that of impact and rubbing rather than that of metal cutting.

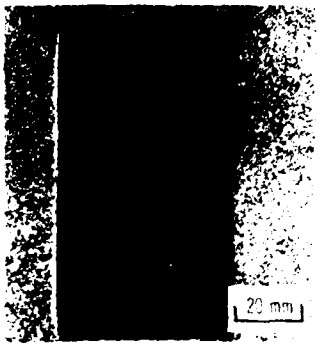

(a) Overview of rub showing smeared and burned areas.

(b) Scanning electron micrograph view of smeared area.

Figure 11. - Sintered, 21-percent-dense Hastelloy-X fibermetal after rub interaction against one rounded Ti-6Al-4V blade tip. Blade tip velocity, 114 m/sec; incursion rate, $25 \cdot 10^{-6}$ m/sec.

Details of the contact geometry at the blade tip leading edge are shown in figure 14. The object of considering the contact geometry on such a detailed level is to develop a model predicting blade tip-seal interface loads and frictional energy dissipation rates. This model will then be compared with the results of the previous section. It is recognized that the interpretation of the force component measurements must be qualified because of the low natural frequency of the radial load transducer. The period of contact of the blade tip with the seal material specimen is short as compared with the natural period of oscillation of the seal material specimen support and load transducer. Therefore

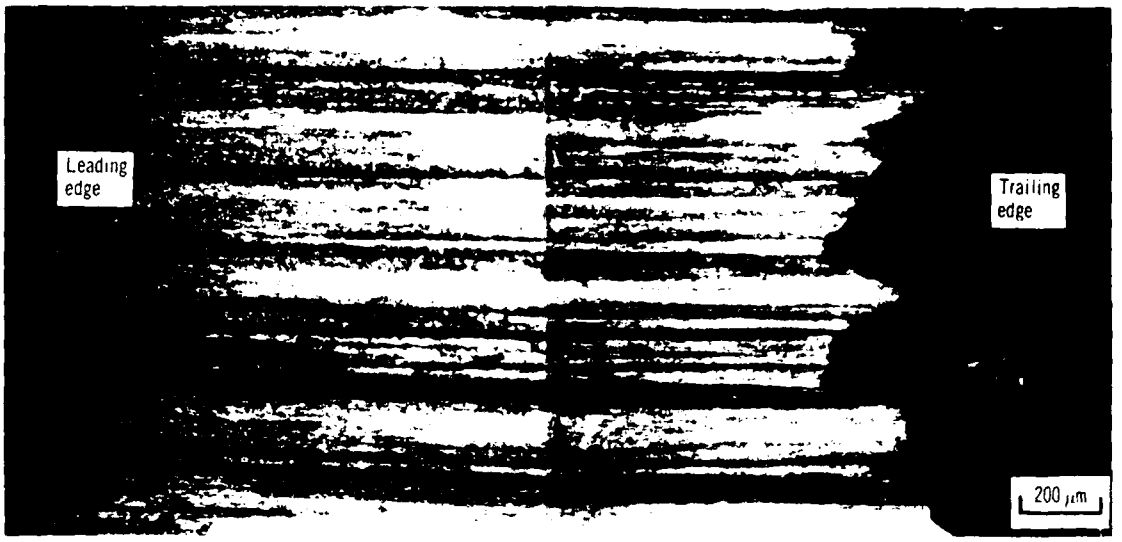

Figure 12. - Rounded Ti-6Al-4V blade tip after rub interaction against 21-percent-dense, sintered Hastelloy-X fibermetal. Blade tip velocity, 114 m/sec; incursion rate, 25×10^{-6} m/sec.

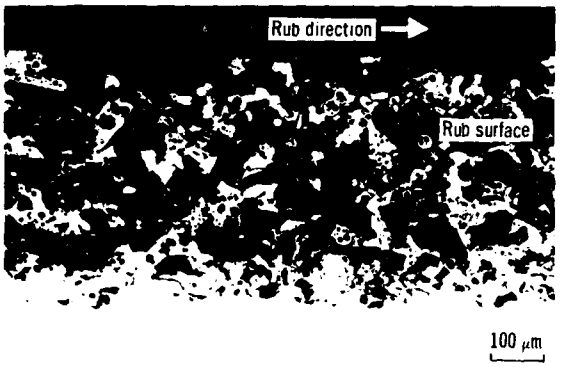

Figure 13. - Metallographic section through rub groove on plasma-sprayed Ni - 25-percent graphite after interaction with thin Ti-6Al-4V blade tips. Blade tip velocity, 114 m/sec; incursion rate, 25×10^{-6} m/sec.

considerable distortion in the load signal will result and some dynamic radial motion of the specimen will be superimposed on the intended incursion motion. These considerations are treated in some detail in appendix A.

In essence the model considers that the "bite per blade" D is accommodated as an impulse step whereby the seal material is very rapidly displaced in a sudden compressive load event. In terms of incursion rate and rotating speed, D is given by

$$D = \frac{2\pi\dot{\Delta}}{\omega N} \tag{2}$$

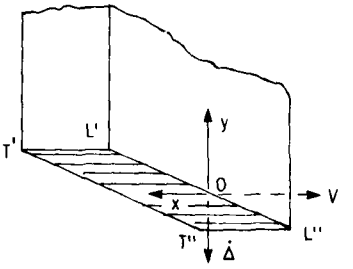

(a) View of blade rub surface L'L''T''T' moving with velocity V and rate of incursion $\dot{\Delta}$ relative to seal material.

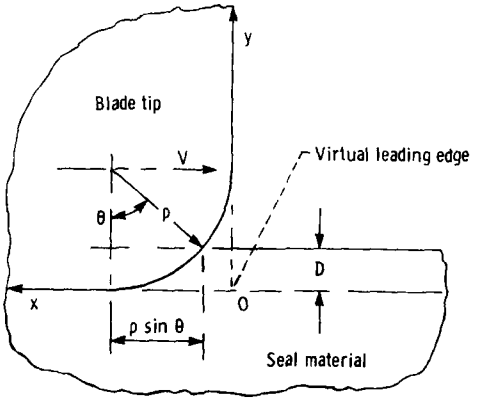

(b) Highly magnified mass section through leading edge L'L'' showing radius of curvature ρ and its geometrical relation to D.

Figure 14. - Blade rub surface.

It may also be expressed in terms of the leading-edge geometry as

$$D = \rho(1 - \cos\theta) \tag{3}$$

The impulse time, that is, the time in which rapid compressive displacement of the seal material takes place, is then given by

$$\Delta t = \frac{\rho \sin\theta}{V} = \frac{\rho\left[2(D/\rho) - (D/\rho)^2\right]^{1/2}}{V} \tag{4}$$

where V is the blade tip velocity ωr. Combining equations (2) and (4) gives the average rate of surface displacement during the impulse step as

$$\frac{D}{\Delta t} = \frac{2\theta\dot{\Delta}r}{N\rho\left[2(D/\rho) - (D/\rho)^2\right]^{1/2}} \tag{5}$$

A simplistic one-dimensional treatment of the impulse step propagating through the seal material (ref. 9) results in an estimate of the average stress σ_1 imposed on the blade tip leading edge:

$$\sigma_1 = \frac{E}{a}\frac{D}{\Delta t} = \frac{E}{a}\frac{2\pi\dot{\Delta}r}{N\rho\left[2(D/\rho) - (D/\rho)^2\right]^{1/2}} \tag{6}$$

The complete blade tip loading consists of two major contributions. First, there is the leading-edge reaction given by equation (6). In addition to the leading-edge reaction there is a distributed load over the remaining tip surface, analogous to the loading on a tool flank surface during a metal cutting operation. Together the two contributions can be expressed as

$$F_r = W\rho a_1 \sin\theta + W\int_{\rho\sin\theta}^{l} \sigma(x)\,dx \tag{7}$$

where W is the width (perpendicular to the sliding direction) of the blade tip, $\sigma(x)$ is the local radial compressive stress at any point x between the beginning of the blade tip flat surface and the trailing edge, and l is the distance from the leading edge to the trailing edge.

An approximate form of $\sigma(x)$ can be obtained by extending the one-dimensional impulse step treatment applied to the leading edge. As the blade tip passes over an element of seal surface material that has been displaced, the impulse propagates further into the seal material. At any position x behind the leading edge, the elapsed time for propagation is x/V, and the propagation distance is ax/V. Therefore $\sigma(x)$ can be written as

$$\sigma(x) = E\frac{DV}{ax} \qquad \text{for } x \geq \rho\sin\theta \tag{8}$$

and equation (7) reduces to (appendix B):

$$F_r = W\rho\sigma_1 \sin\theta\left(1 + \ln\frac{l}{\sin\theta}\right)$$

$$= W\frac{E}{a}DV\left(1 + \ln\frac{l}{\rho\sin\theta}\right) \tag{9}$$

When the conditions for a 10-blade-tip rub interaction against 21-percent-dense Hastelloy-X fibermetal ($E = 968$ MN/m^2 and a is calculated to be 1030 m/sec) at 115 m/sec are substituted into equations (6) and (9), σ_1 turns out to be 3.8 MN/m^2 and F_r is about 0.25 newton. The predicted radial load is obviously much lower than the measured radial loads, and the discrepancy is not accounted for by the dynamic response of the cantilever load cell (appendix A).

The most probable source of discrepancy is the assumption that $D = 2\pi\dot{\Delta}/\omega N$; that is, with each blade encounter material is worn from the seal surface to a depth D. More likely, seal material removal does not occur until σ_1 reaches a critical level, with the actual value of D increasing until that critical stress level is reached. In the meantime densification of the seal material just below the surface occurs, resulting in a smeared rub surface. For a given impulse step D, σ_1 is approximated by

$$\sigma_1 = \frac{E}{a}\frac{VD^{1/2}}{a\sqrt{2\rho}} \tag{10}$$

In the absence of blade tip leading-edge wear σ_1 approaches a value at which rapid plastic flow of the smeared seal material surface layer would be expected (100 to 150 MN/m^2, assuming the rub surface temperature approaches 900° C as indicated by visible orange glowing) after 500 to 1000 blade passes. At this point predicted radial loads (eq. (9)) do indeed approach the measured values. However, D and ρ are of similar magnitude after 500 to 1000 passes, and the threshold for metal cutting in the smeared layer is approached. Considering the low mechanical strength of the porous substrate below the smeared layer, the possibility of periodic tearing of the substrate and disruption of the smeared layer exists and is in fact noted in table I and shown in figure 3. In effect, the stresses associated with rapid removal of metal from the smeared rub surface exceed the cohesive strength of the substrate. This periodic disruption of the smeared rub surface and tearing of the substrate are the causes of the load fluctuations noted in figures 2 and 6. Significantly,

the rise time for the large peaks (0.25 to 0.50 sec) is consistent with the number of blade passes (10-blade-tip case) required to approach the critical σ_l level for large-scale plastic flow of the smeared layer.

The sharper load peaks and more intermittent loading noted when one standard blade tip was used rather than 10 (fig. 2) are both consistent with the rub interaction model proposed. As the critical value of σ_l is approached, seal material is removed in a more sudden and severe event than is the case for 10 blade tips, because of the ten times larger "bite per blade" incursion depth increment. The severity of the event often removes seal material to a depth greater than the nominal incursion depth and results in periodic zero blade tip loading.

Except for somewhat higher blade tip wear the blade tip loading and general rub behavior of the thin blade tips were similar to those of the standard blade tips, as can be seen in table I and figure 6. From the proposed model these observations were expected. Equation (9) predicts radial loads only about 10 to 15 percent lower than those predicted for the 3.2-millimeter-thick blade tips. Such differences are not likely to be resolved in these experiments. The dominant blade tip feature governing rub behavior of both the thick and thin blade tips is the leading-edge sharpness, which was at least initially the same for both cases.

Results for the rounded blade tips differed markedly from those for the standard-sharpness blade tips, especially with regard to the loading pattern (fig. 10). Combining equations (6) and (9) while noting that because of the cylindrical tip geometry for the rounded blade tips $l = \rho \sin \theta$ makes it apparent that σ_l never approached its critical value. In fact at the final measured load level of 5 newtons the predicted value for σ_l was approximately 1.3 MN/m^2 (200 psi). Under these conditions the seal material was simply densified and smeared during each blade pass. Extensive plastic flow and plowing of the smeared layer would not be expected, and metal cutting conditions were never reached. In no instance was tearing and mechanical disruption of the smeared surface observed. Rub equilibrium was reached when the wear rate of the smeared layer equalled the rate of densification. The situation for the deliberately rounded blade tips pertains in general to conditions under which extensive blade tip leading-edge wear occurs.

Although the test matrix applied to the four seal materials listed in table II was not as extensive as that applied to the sintered Hastelloy-X fibermetal, some interesting patterns were noted in the results. The observation was made that for sintered nickel-chromium and plasma-sprayed nickel-graphite smearing occurred at most to a small degree. Peak loads were higher for single-blade-tip tests than for 10-blade-tip tests, which is consistent with the model proposed herein. It is concluded that the behavior of these materials in terms of blade tip loading is generally similar to that of the sintered Hastelloy-X fibermetal. Rubs were less severe, however, because of the reduced smearing tendency—a consequence of particle shape and bonding (ref. 3).

For the rather dense plasma-sprayed aluminum-silicon-polyester and aluminum-graphite systems, however, the effect of the number of blade tips is not easily understood. Perhaps in the single-blade-tip experiments conditions of metal cutting were reached and led to reduced blade tip loading in comparison rubbing conditions. Another factor is the rule of seal material transfer to the blade tips. Transfer was consistently observed in the aluminum-based systems under single-blade-tip test conditions. Transferred aluminum might have provided a "soft tip" condition during single-blade-tip rubs and masked the validity of the proposed model.

Conclusions

From the rub interaction experiments conducted against sintered Hastelloy-X fibermetal and other seal materials, the following conclusions were reached:

1. Contact was very unsteady for all experiments conducted with blade tips having sharp (5-μm radius of curvature) leading edges.

2. In all experiments contact was predominantly rubbing rather than cutting. For sharp-blade-tip experiments cutting may occur and is accompanied by tearing of the substrate for the case of fibermetal seal materials.

3. Cutting only occurred after long periods of rub interaction during which the accumulated incursion depth increment approached the blade tip radius of curvature.

4. The peak loads measured and the unsteady nature of the blade tip-seal contact are consistent with a proposed blade tip loading model. The proposed model is based on the propagation of an elastic stress wave through the seal material as the seal material is dynamically compressed by the blade tip leading edge.

Lewis Research Center
National Aeronautics and Space Administration
Cleveland, Ohio, October 28, 1980

Appendix A

Load Cantilever Response

The dynamic response of the load cell to blade tip loading can be approximated by considering the cantilevered load cell, with its effective spring constant and mass, as an undamped harmonic system. If the period of impulse (duration of blade tip contact with the specimen) is τ, during τ the cantilever displacement $y(t)$ is given by (ref. 10)

$$y(t) = \int_0^t f(\xi) g(t-\xi)\, d\xi \tag{A1}$$

where $f(\xi)$ is the impulse function

$$f(\xi) = F_r \tag{A2}$$

and $g(t)$ is given by

$$g(t) = \frac{1}{m\omega_n} \sin\, \omega_n t \tag{A3}$$

In this equation ω_n is the natural frequency of the cantilever, experimentally determined to be 2400 rad/sec. Equation (A1) becomes

$$y(t) = \frac{F_r}{m\omega_n} \int_0^t \sin\, \omega_n(t-\xi)\, d\xi$$

Therefore

$$Ky(t) = F_r(1 - \cos\, \omega_n t) \tag{A4}$$

where $Ky(t)$ is the experimentally measured load at time t during blade contact and F_r is the actual load. For time $t > \tau$ (after blade contact)

$$g(t) = -\frac{F_r}{m\omega_n} \int_\tau^t \sin\, \omega_n(t-\xi)\, d\xi + \frac{F_r}{K}(1 - \cos\, \omega_n t)$$

So

$$Ky(t) = F_r[\cos\, \omega_n(t-\tau) - \cos\, \omega_n t] \tag{A5}$$

The duration of a blade contact τ is about 3×10^{-4} second. Calculated values of $Ky(t)$ compared with F_r for various times during and after a blade contact are summarized in figure 15. Although apparent loads are never more than about 70 percent of actual contact load, the right order of magnitude of the actual load is detected.

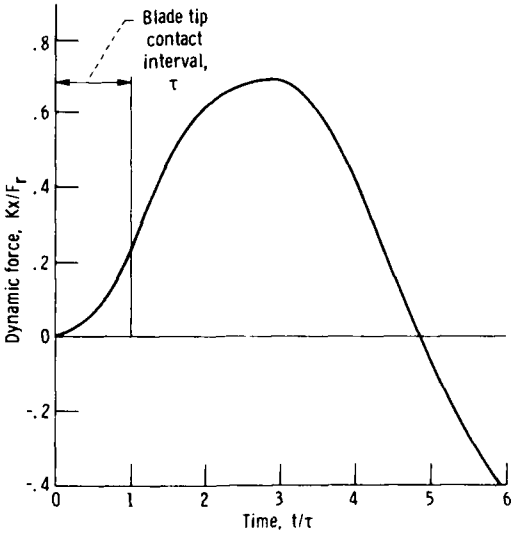

Figure 15. - Dynamic (undamped) response of cantilever load cell.

Appendix B

Blade Tip Load Derivation

The total blade tip radial load was expressed in the text as

$$F_r = W\rho\sigma_1 \sin\theta + W\int_{\rho\sin\theta}^{l} \sigma(x)\, dx \tag{7}$$

At any distance x behind the leading-edge cylinder of contact

$$\sigma(x) = E\frac{DV}{ax} \tag{8}$$

Then

$$F_r = W\rho\sigma_1 \sin\theta + W\frac{EDV}{a}\int_{\rho\sin\theta}^{l} \frac{1}{x}dx \tag{A5}$$

where l is the blade tip thickness. From equation (6)

$$\sigma_1 = \frac{ED}{a\,\Delta t}$$

and from equation (4)

$$\Delta t = \frac{\rho \sin\theta}{V}$$

Hence

$$\frac{EDV}{a} = \rho\theta_1 \sin\theta$$

and equation (16) becomes

$$F_r = W\rho\sigma_1 \sin\theta\left(1 + \int_{\rho\sin\theta}^{l} \frac{1}{x}dx\right)$$

$$= W\rho\sigma_1 \sin\theta\left(1 + \ln\frac{l}{\rho \sin\theta}\right)$$

References

1. Roelke, Richard J.: Miscellaneous Losses. Turbine Design and Application, A. J. Glassman, ed., NASA SP-290, 1973, pp. 125-148.
2. Hauser, Cavour H.; et al.: Compressor and Turbine Technology. Aeronautical Propulsion, NASA SP-381, 1975, pp. 229-288.
3. Bill, R. C.; and Wisander, D. W.: Friction and Wear of Several Compressor Gas Path Seal Materials. NASA TP-1128, 1978.
4. Bill, R. C.; and Shiembob, L. T.: Friction and Wear of Sintered Fibermetal Abradable Seal Materals. NASA TM X-73650, 1977.
5. Schwab, R. C.: Program to Develop Sprayed, Plastically Deformable Compressor Shroud Seal Materials. (ITPR-1, General Electric Co.; NASA Contract NAS3-20054.) NASA CR-159741, 1979.
6. Bill, R. C.; and Shiembob, L. T.: Some Considerations of the Performance of Two Honeycomb Gas Path Seal Material Systems. AVRADCOM-TR-79-33, NASA TM-81398, 1980.
7. Bowden, F. P.; and Tabor D.: The Friction and Lubrication of Solids. Part II, Oxford Clarendon Press (London) 1964, p. 347.
8. Albrecht, P.: New Developments in the Theory of the Metal-Cutting Process. Part I. The Ploughing Process in Metal Cutting. J. Eng. Ind., vol. 82, no. 4, Nov. 1960, pp. 348-358.
9. Timoshenko, S.; and Goodier, J. N.: Theory of Elasticity. Third ed. McGraw-Hill Book Co., 1970, pp. 492-497.
10. Thomson, W. T.: Vibration Theory and Applications. Prentice-Hall, Inc., 1965, pp. 99-109.

1. Report No. NASA TP-1835 AVRADCOM TR 80-C-19	2. Government Accession No. AD-A097 600	3. Recipient's Catalog No.
4. Title and Subtitle EFFECTS OF GEOMETRIC VARIABLES ON RUB CHARACTERISTICS OF Ti-6Al-4V		5. Report Date April 1981 6. Performing Organization Code 505-32-42
7. Author(s) Robert C. Bill, Jan Wolak, and Donald W. Wisander		8. Performing Organization Report No. E-449
9. Performing Organization Name and Address National Aeronautics and Space Administration and AVRADCOM Research and Technology Laboratories Cleveland, Ohio 44135		10. Work Unit No. 11. Contract or Grant No.
12. Sponsoring Agency Name and Address National Aeronautics and Space Administration Washington, D.C. 20546 and U.S. Army Aviation Research and Development Command, St. Louis, Mo. 63166		13. Type of Report and Period Covered Technical Paper 14. Sponsoring Agency Code

15. Supplementary Notes

Robert C. Bill, AVRADCOM Research and Technology Laboratories; Jan Wolak, University of Washington, Seattle, Washington; Donald W. Wisander, Lewis Research Center

16. Abstract

Experiments simulating rub interactions between Ti-6Al-4V blade tips and various seal materials were conducted. The number of blade tips and the blade tip geometry were varied to determine their effects on rub forces and on wear phenomena. Contact was found to be quite unsteady for all blade tip geometries except for those incorporating deliberately rounded blade tips. The unsteady contact was characterized by long periods of rubbing contact and increasing blade tip load that terminated in sudden rapid metal removal, sometimes accompanied by tearing and disruption of porous seal material under the rub surface. A model describing the blade tip loading is proposed and is based on the propagation of an elastic stress wave through the seal material as the seal material is dynamically compressed by the blade tip leading edge.

17. Key Words (Suggested by Author(s))	18. Distribution Statement		
Wear; Rotor blades; Titanium alloys; Seals (stoppers)	Unclassified - unlimited Subject Category 26		
19. Security Classif. (of this report) Unclassified	20. Security Classif. (of this page) Unclassified	21. No. of Pages 20	22. Price* A02

* For sale by the National Technical Information Service, Springfield, Virginia 22161

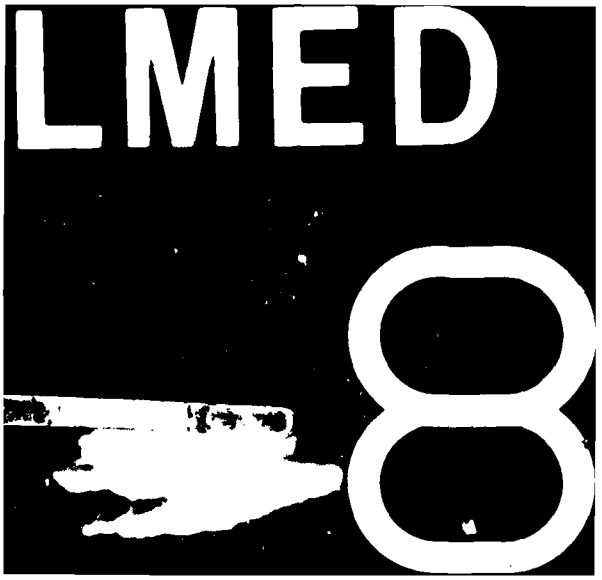
LMED
8